

Irrigant flow within a prepared root canal using various flow rates: a Computational Fluid Dynamics study

C. Boutsoukis¹, T. Lambrianidis¹ & E. Kastrinakis²

¹Department of Endodontology, Dental School; and ²Chemical Engineering Department, School of Engineering, Aristotle University of Thessaloniki, Thessaloniki, Greece

Abstract

Boutsoukis C, Lambrianidis T, Kastrinakis E. Irrigant flow within a prepared root canal using various flow rates: a Computational Fluid Dynamics study. *International Endodontic Journal*, 42, 144–155, 2009.

Aim To study using computer simulation the effect of irrigant flow rate on the flow pattern within a prepared root canal, during final irrigation with a syringe and needle.

Methodology Geometrical characteristics of a side-vented endodontic needle and clinically realistic flow rate values were obtained from previous and preliminary studies. A Computational Fluid Dynamics (CFD) model was created using FLUENT 6.2 software. Calculations were carried out for five selected flow rates (0.02–0.79 mL sec⁻¹) and velocity and turbulence quantities along the domain were evaluated.

Results Irrigant replacement was limited to 1–1.5 mm apical to the needle tip for all flow rates tested. Low-Reynolds number turbulent flow was detected near the needle outlet. Irrigant flow rate affected significantly the flow pattern within the root canal.

Conclusions Irrigation needles should be placed to within 1 mm from working length to ensure fluid exchange. Turbulent flow of irrigant leads to more efficient irrigant replacement. CFD represents a powerful tool for the study of irrigation.

Keywords: computational fluid dynamics, flow rate, irrigation, needle.

Received 16 June 2008; accepted 14 October 2008

Introduction

Irrigation of root canals with antibacterial solutions is considered an essential part of chemo-mechanical preparation (Haapasalo *et al.* 2005). Irrigation is complementary to instrumentation in facilitating removal of bacteria, debris and necrotic tissue (Lee *et al.* 2004a), especially from areas of the root canal that have been left unprepared by mechanical instruments (Gulabivala *et al.* 2005). The effectiveness of irrigation relies on mechanical flushing and the ability of irrigants to

eliminate bacteria (Gulabivala *et al.* 2005) and dissolve tissue (Lee *et al.* 2004a).

Efficient debridement and successful destruction of microorganisms even depend on the irrigant's penetration along the full length of the canal and on irrigant exchange (Salzgeber & Brilliant 1977, Druttman & Stock 1989). Consequently, irrigation dynamics should be considered when evaluating the effect of an irrigant on root canal contents (Gulabivala *et al.* 2005). The penetration of the irrigant and the flushing action created by irrigation are dependent not only on the anatomy of the root canal system, but also on the system of delivery, the depth of placement, and the volume and fluid properties of the irrigant (Ram 1977, Abou-Rass & Piccinino 1982, Moser & Heuer

Correspondence: Christos Boutsoukis, 29, Kimis Str. 551 33 Thessaloniki, Greece (Tel.: +302310427813; fax: +302310999639; e-mail: chb@dent.auth.gr).

1982, Chow 1983, Kahn *et al.* 1995, Lee *et al.* 2004a, Gulabivala *et al.* 2005, Sedgley *et al.* 2005).

Conventional irrigation with a syringe and needle remains widely accepted (Ingle *et al.* 2002, Peters 2004). Classical endodontic handbooks refer to hand irrigation as a simple procedure (Ingle *et al.* 2002) and provide general guidelines in order to maximize irrigation efficiency and avoid extrusion of irrigant to the periapical tissue (Ruddle 2002, Wesselink & Bergenholtz 2004). However, in a recent study (Boutsioukis *et al.* 2007a) wide variations were found amongst endodontists concerning the irrigation procedure.

Although poorly studied, there is a general uncertainty about the efficiency of irrigation in the narrow, most apical part of the canal (Senia *et al.* 1971, Vande Visse & Brilliant 1975, Ram 1977, Haapasalo *et al.* 2005). It has been argued that the difficulty in reaching the most apical region of the canal with large volumes of fresh irrigant may result in poorer performance of the irrigant (Druttman & Stock 1989, Haapasalo *et al.* 2005), but only speculation exists over the extent these factors influence the development of currents within the canal (Ram 1977, Abou-Rass & Piccinino 1982, Chow 1983, Druttman & Stock 1989, Sedgley *et al.* 2005, Zehnder 2006).

Earlier attempts to evaluate the flow of irrigants within the canal were based on macroscopic observations (Goldman *et al.* 1976, Krell *et al.* 1988), frequently of the displacement of a coloured dye by the delivered irrigant (Kahn *et al.* 1995), or on radiographic appearance of a partly radiopaque solution (Ram 1977, Salzgeber & Brilliant 1977, Abou-Rass & Piccinino 1982). Although these early attempts to evaluate the flow of irrigants developed our current knowledge regarding irrigation, they only described macroscopic events, and were frequently limited by the relatively poor ability of radiographs (Salzgeber & Brilliant 1977) or visual examination to detect the dynamics of fluid movement.

Recently applied methods such as real-time imaging of bioluminescent bacteria (Sedgley *et al.* 2004, 2005, Falk & Sedgley 2005, Nguy & Sedgley 2006) and studying the mechanical effect of irrigations on artificially placed debris in simulated irregularities with the aid of stereoscopic microscopes and digital images (Lee *et al.* 2004a,b, van der Sluis *et al.* 2005, 2006) have overcome these limitations and provided valuable data about the effect of irrigation on microbes and debris. However, these methods have provided little insight to the aetiology of these effects, that is, the flow pattern developed within the needle and root canal. Hsieh *et al.*

2007 showed dynamic flow conditions during irrigation with thermal image analysis. This method provided data on the flow of an irrigant within a root canal *ex vivo*. However, it may be necessary to assess whether fluid flow monitoring is affected by the simultaneous heat flux from the warm fresh irrigant to the cooler irrigant within the canal and the canal walls. The possibility that heat flux may occur at a rate similar to the irrigant flow rate cannot be discarded. In addition, the artificial change of the normal irrigant and root canal temperature could result in altered physical properties, such as decreased viscosity, affecting the results.

Computational Fluid Dynamics (CFD) represents a powerful tool to investigate flow patterns and physical and chemical phenomena by mathematical modelling and computer simulation (Tilton 1999, Arvand *et al.* 2005). Despite the fact that CFD was originally developed for industrial and engineering purposes, in recent years applications in the biomedical field have also attracted considerable attention (Xu *et al.* 2006), aided by the increasing power of computers (Politis *et al.* 2007). CFD has been previously applied to investigate several problems in the cardiovascular and the respiratory system (Pekkan *et al.* 2005, Yoganathan *et al.* 2005, Corno *et al.* 2006, Jung *et al.* 2006, van Tricht *et al.* 2006, Xu *et al.* 2006, Yang *et al.* 2006a,b, Politis *et al.* 2007).

The aim of this study was to investigate the effect of irrigant flow rate on the flow pattern within a prepared root canal, during final irrigation with a syringe and needle using a CFD model.

Materials and methods

Analysis of model geometry

The shape of the selected needle (30G KerrHawe Irrigation Probe, KerrHawe SA, Bioggio, Switzerland) was obtained through images from Stereoscopic Microscope (Fig. 1a). These images were calibrated using the needle external diameter, known from a previous study (Boutsioukis *et al.* 2007b). The cross-sectional areas and the perimeters were then obtained through standard computer image analysis with AutoCAD 2006 software (AutoDesk, San Rafael, CA, USA). Needle length was determined with precision calipers (accuracy 0.05 mm). These data were used to plot the needle perimeter (Fig. 1b).

The root canal was simulated as a geometrical frustum of cone 19 mm in length, with a diameter of

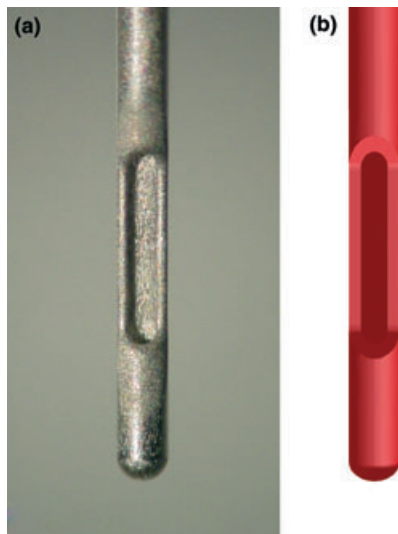


Figure 1 (a) Part of the 30-G side vented needle (KerrHawe Irrigation Probe, KerrHawe SA, Bioggio, Switzerland) containing the needle outlet. (b) The same part of the needle-model.

0.45 mm (ISO size 45) at full working length, and a diameter of 1.59 mm at the canal orifice, 19 mm coronally. This shape is consistent with final canal shaping with a rotary-driven Ni-Ti size 45 .06 taper instrument (K3, Sybron Endo, Orange, CA, USA) used

at full working length in order to standardize the canal shape, as described in a previous study (Boutsoukis et al. 2007a). The apical terminus of the root canal, was also simulated as an inverted frustum of cone with a length of 0.5 mm connected with the original frustum, to simulate the effect of a patency file used during root canal preparation. The diameter of the apical constriction was 0.3 mm and the diameter of the apical foramen 0.35 mm (Fig. 2). Apical root canal geometry was constructed according to data provided in a recent study (Ponce & Fernandez 2003), in order to simulate the shape of a maxillary central incisor's root canal. The needle was considered to be placed 3 mm short of the working length, centered within the canal and immovable.

Mesh generation

The pre-processor software Gambit 2.2 (Fluent Inc., Lebanon, NH, USA) was used to build the 3-D geometry and the mesh. Due to existing symmetries, only half of the geometry was studied (Fig. 3). A structured hexahedral mesh was constructed with higher density in the areas where high gradients of velocity and turbulence were anticipated, namely near the needle exit.

A grid-independency check was performed to determine the minimum number of computational cells

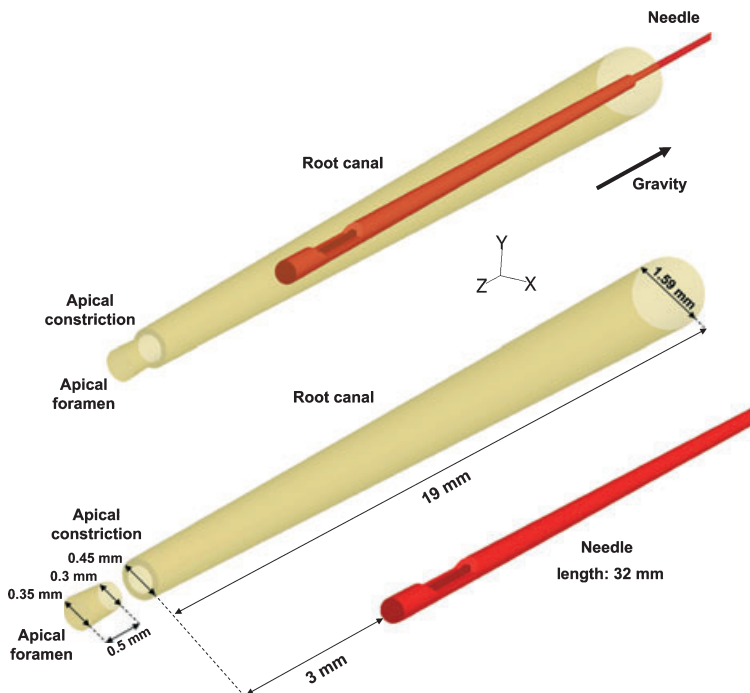
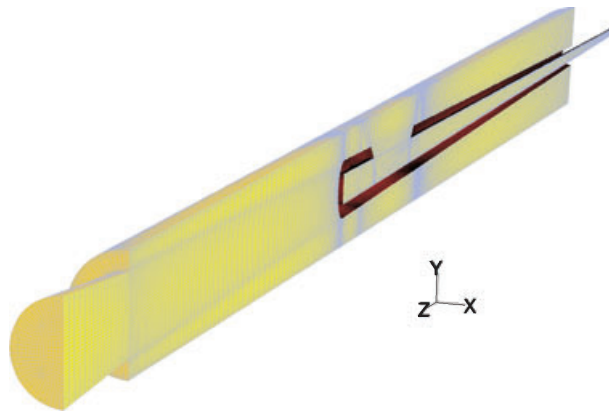


Figure 2 Geometrical characteristics of the root canal model used.

Figure 3 View of the computational mesh in the apical part of the canal. Only half of the domain was studied, due to existing symmetries. The mesh displayed is coarser than the one employed in the calculations, and is only used for illustration purposes.



required for a grid-independent flow simulation and ensure reasonable use of computational resources. A coarse mesh (369 688 cells) was initially constructed. Preliminary simulations were performed with identical boundary and initial conditions, with inlet velocity of 36 m sec^{-1} , corresponding to Case E (Table 1). Velocity as well as turbulence quantities were examined at several cross-sections along the domain. The initial mesh was gradually refined in order to improve accuracy until further refinement produced insignificant change in the results. The final mesh consisted of 1 279 856 cells (Mean cell volume $6.4885 \cdot 10^{-6} \text{ mm}^3$). The mesh resolution satisfied the near-wall mesh guidelines proposed for the selected turbulence model. This mesh was used for all cases studied.

Boundary and operating conditions

Boundary conditions were set in order to simulate a final irrigation under routine clinical conditions. No-slip boundary conditions were applied to the solid surfaces, which are the walls of the canal and of the needle, under the hypothesis of rigid, smooth and impermeable walls. A symmetry boundary condition was used for the lateral side of the flow domain, at the

z - y plane. The fluid flows in from the distal end of the needle and out from the orifice of the root canal. The canal and needle are assumed to be completely filled with the irrigant.

A velocity inlet boundary condition was selected for the entrance of the needle lumen, distally to the root canal. A constant axial irrigant velocity with a flat velocity profile was imposed at the inlet for each of the five cases studied (Table 1). The range of clinically realistic irrigant flow rates was determined in a previous study (Boutsioukis *et al.* 2007a). Flow rate values were converted to inlet velocity values. Turbulence intensity (ratio of the magnitude of the RMS turbulent fluctuations to the inlet velocity) at the inlet was set to 5% and hydraulic diameter was defined as equal to the actual needle internal diameter. A pressure outlet boundary condition was imposed at the root canal orifice to allow flow of the irrigant away from the domain. Atmospheric pressure was assumed at the outlet.

The irrigation fluid, sodium hypochlorite 1% aqueous solution, was modelled as an incompressible, Newtonian fluid, an assumption that is generally accepted for pure water and sparse aqueous solutions (Tilton 1999), with density, ρ , equal to 1.04 g cm^{-3} and viscosity, μ , $0.986 \cdot 10^{-3} \text{ Pa}\cdot\text{s}$. Irrigant density and viscosity were selected to match standard values reported in the literature (Guerisoli *et al.* 1998). Gravity was included in the flow field at the direction of the negative- z axis.

Table 1 Inlet conditions for the five cases studied

Case	Inlet velocity (m sec^{-1})	Irrigant flow rate (mL sec^{-1})	Reynolds number at the needle inlet
A	1	0.02	177
B	6	0.14	1063
C	12	0.26	2126
D	24	0.53	4253
E	36	0.79	6379

Initial conditions

The domain was initialized with the irrigant at 50% of the inlet z -velocity, whilst x -velocity, y -velocity and gage pressure were set to zero. Initial values for the

turbulence kinetic energy and turbulence dissipation rate were calculated from the corresponding values at the needle inlet, in order to avoid a 'cold start'.

Solver setup

The commercial CFD code FLUENT 6.2 (Fluent Inc., Lebanon, NH, USA), was used to set up and solve the problem and to analyze the results. The numerical solution method uses a finite volume approach applied to an unstructured mesh. A steady and isothermal flow was assumed. The governing time-averaged, three-dimensional, incompressible Reynolds - Averaged Navier-Stokes (RANS) equations were solved by a segregated implicit iterative solver. A low-Reynolds RNG - modified $k - \epsilon$ turbulence model was used for all cases. All transport equations were discretized to be at least second-order accurate in space. The convergence criterion was at least 10^{-8} of the maximum scaled residuals. Pressure, velocity and turbulence quantities in selected areas of the flow domain were also monitored to ensure adequate convergence. Computations were carried out on a Windows XP Personal Computer with a 3 GHz single Intel Pentium IV Hyper-threading processor and 2 GB of RAM.

A series of computations for five different inlet velocities were performed (Table 1). Results were analyzed and flow fields computed for the five cases were compared.

Lagrangian particle tracking was performed as a post-processing operation, in which the routes of massless particles were tracked throughout the flow domain after release from the inlet of the needle.

Results

The effect of inlet needle velocity appeared to be highly significant in determining the flow field within the canal. Lower velocities and similar flow patterns were observed in the middle and coronal third of all cases, regardless of inlet velocity, indicating a laminar flow. Differences were mainly noticed in the apical third.

Overall the highest velocities were observed within the needle lumen (Fig. 4). Velocities dropped by an order of magnitude at the needle outlet, due to the relatively sudden expansion of the area downstream of the outlet. Maximum irrigant velocities within the root canal were primarily observed in the vicinity of the needle outlet. The velocity magnitude increased as the irrigant inlet velocity increased, as expected.

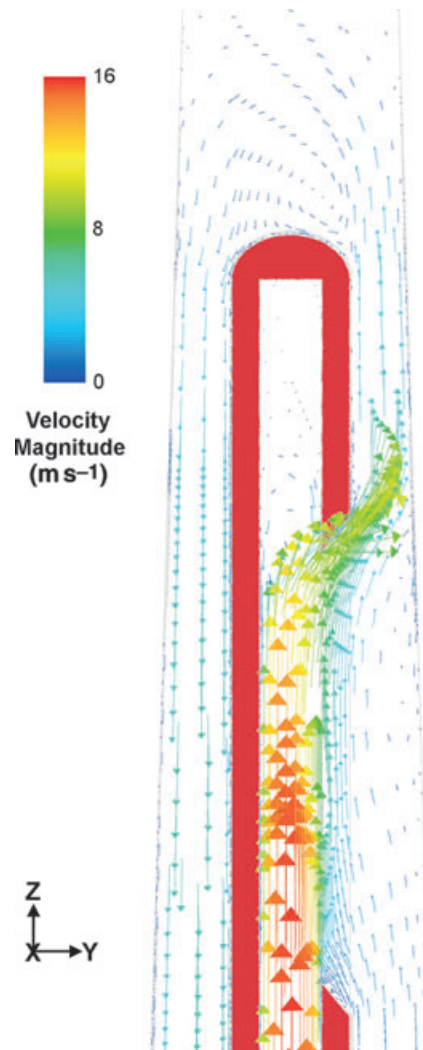


Figure 4 Velocity vectors along the symmetry plane ($z-y$) in the area of the needle outlet coloured by velocity magnitude for a representative case (Case C). The needle wall is coloured red.

As the irrigant approached the needle outlet, it primarily followed the main flow stream (Fig. 4) towards the root canal. Irrigant within the distal part of the needle, just apically to the outlet, exhibited an almost stagnant behaviour in all cases. A jet of irrigant was formed at the needle outlet, directed towards the apex with a divergence of approximately 30 degrees. This jet was more intense and obvious in higher velocity cases. Irrigant flowing out of the needle followed a curved path around the needle tip, where a small anticlockwise vortex was observed, and was finally directed towards the canal orifice. In the area

just coronal to the needle outlet low irrigant velocities were observed and reverse flow regions were formed, where irrigant flows towards the apex rather than the orifice (Fig. 4).

According to the turbulence intensity and turbulent viscosity ratio (ratio of the turbulent viscosity of the fluid computed using the turbulence model to the laminar viscosity) distribution, mostly laminar flow was developed in cases A and B, whilst increasing amounts of low Reynolds turbulence was developed within the needle lumen, near the needle outlet and immediately in front of the needle tip in cases C–E (Fig. 5). No turbulent phenomena were observed coronally to the needle outlet in any of the cases studied.

Stream-lines indicating the route of mass-less particles released downstream from the needle inlet coloured according to velocity magnitude depict the flow of the delivered irrigant in the canal (Fig. 6). The main flow appeared to spread laterally around the needle whilst following a curved path around the needle tip, with limited apical penetration and was finally directed towards the canal orifice. Overall, very limited irrigant replacement could be identified in the apical part of the canal. Increase of the inlet velocity led to more efficient irrigant replacement. Nevertheless, this effect was limited to 1–1.5 mm apically to the needle tip, even

with maximum inlet velocity studied (case E). Particle trajectories verified that irrigant flow was mostly laminar in case A and B, whereas increasing turbulence presented in case C–E, around the needle outlet and immediately apically to the needle tip.

Analysis of the z -component of irrigant velocity along the longitudinal axis of the root canal (z -axis) confirmed the increasing depth of irrigant replacement, which in any case did not exceed 1–1.5 mm apically to the needle tip (Fig. 7).

Discussion

In the present study, irrigant flow in a root canal with various inlet velocities was numerically simulated, using a previously validated commercial CFD code. This paper represents an initial attempt to apply a well-established engineering method to the investigation of an endodontic problem.

Average maxillary central incisor length has been reported to be 23.3 mm (Ingle *et al.* 2002). Nevertheless, due to geometrical simplification, the length of the root canal part that could be modelled as a frustum of cone had to be determined. During a preliminary study, the average length of the root canal of ten randomly selected maxillary central incisors was determined as the distance between the apical foramen and the most

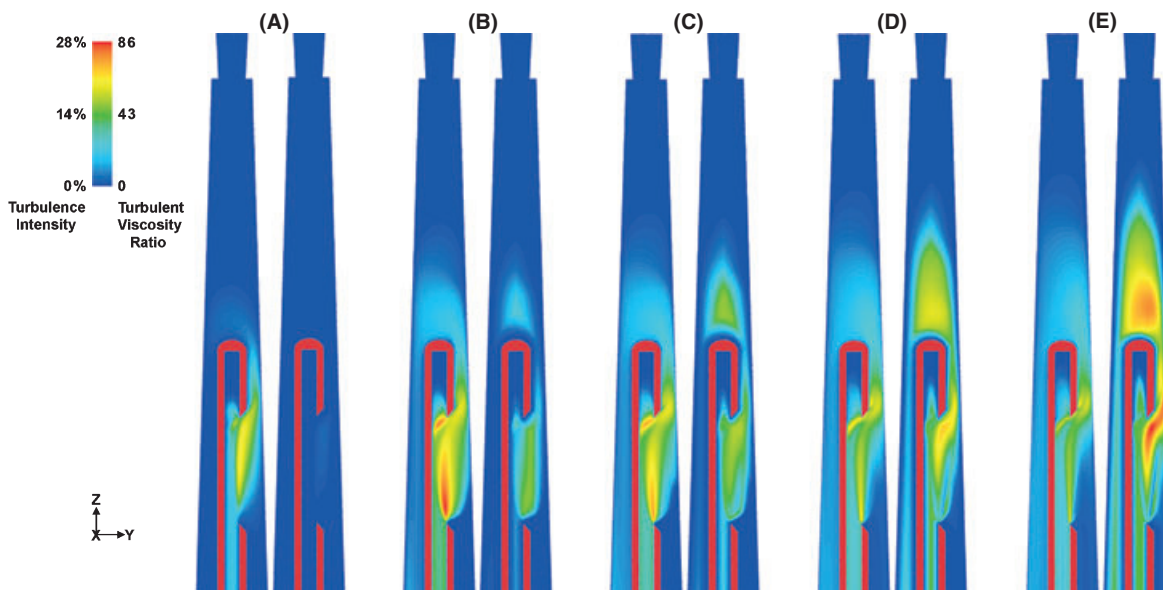


Figure 5 Pairs of contours of turbulence intensity (left) and turbulent viscosity ratio (right) along the symmetry plane (z - y) of the domain for the cases studied. The needle wall is coloured red. Low-Reynolds turbulence was noticed within the needle lumen, near the outlet and immediately in front of the needle tip in cases C–E.

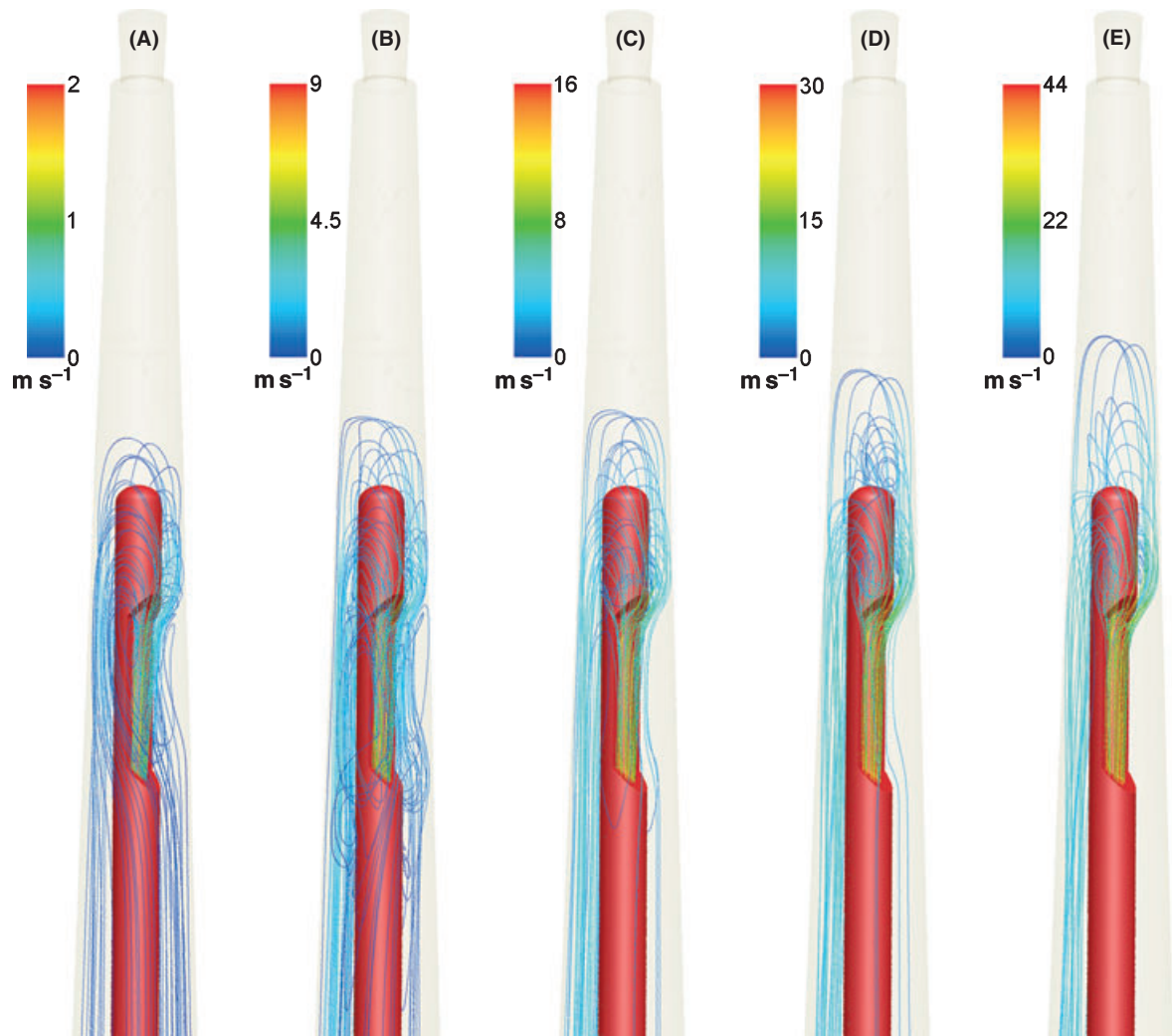


Figure 6 Stream-lines indicating the route of mass-less particles released downstream from the needle inlet and coloured according to velocity magnitude (m s^{-1}). Particle trajectories provide visualization of the fresh irrigant flow.

apical side of the standard access cavity. This resulted in an average length of 19.5 mm.

In the current study, the apical foramen was simulated as an impermeable and rigid wall, due to existing limitations of the model applied. Such an assumption excludes the possibility of irrigant extrusion towards the periapical tissue, an incident that is known to occur clinically and has been associated with forceful delivery of the irrigant (Vande Visse & Brilliant 1975, Ram 1977, Druttman & Stock 1989, Lambrianidis 2001, Lambrianidis *et al.* 2001, Tinaz *et al.* 2005) and with the presence of periapical lesions (Salzgeber & Brilliant 1977). It seems reasonable to assume that extrusion of irrigant takes place if

irrigant pressure at the apical foramen exceeds the back-pressure from the periapical area. Thus, in cases of low irrigant flow rate, when low pressures are anticipated, the assumption of an impermeable wall at the apical foramen may be more realistic than the assumption of zero back-pressure usually employed in extrusion studies (Vande Visse & Brilliant 1975, Lambrianidis *et al.* 2001, Tinaz *et al.* 2005). Yet, in high flow rate cases, tissue back-pressure may be overcome and a certain amount of irrigant could be extruded to the periapical area.

In the present study the root canal was assumed to be completely filled with the irrigant, in order to simplify the model. This assumption may not be

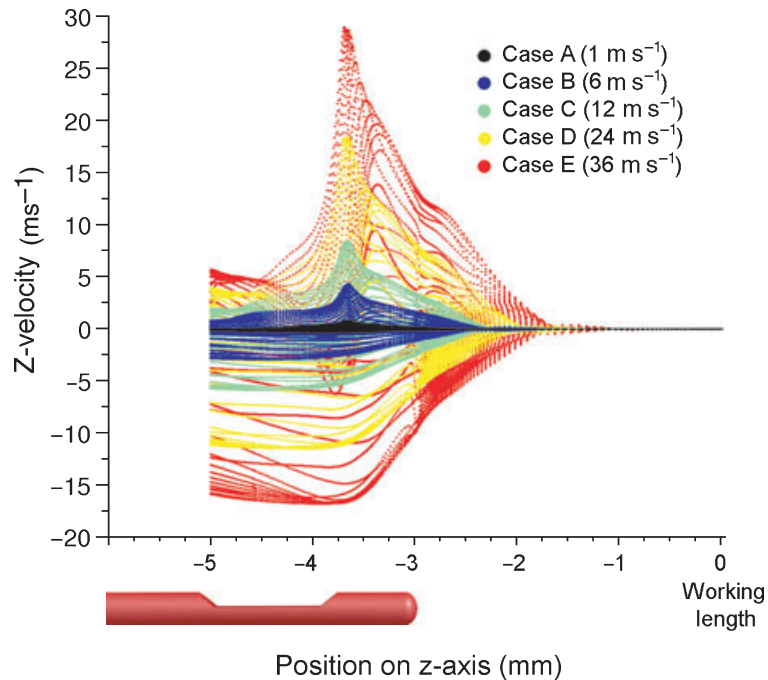


Figure 7 Distribution of the z-component of irrigant velocity as a function of position on the z-axis (longitudinal axis of the root canal) for the cases studied. The needle position is provided for comparison. Note the increasing depth of irrigant replacement as the inlet velocity is increased, which reaches maximum 1.5 mm apically to the needle tip in case E.

completely realistic, as dentine chips, debris or other fluids may be present in certain areas of the canal. Furthermore, in maxillary teeth there is a possibility of air bubble entrapment in the most apical part of the root canal.

Average flow rate of a fluid (Q) within a pipe (such as the needle lumen) is defined as:

$$Q = U \cdot S$$

where U is the average fluid velocity and S is the area of the cross section of the pipe (Hughes & Brighton 1999). Inlet velocity values for the five cases studied (Table 1) were calculated from flow rate data (Boutsioukis *et al.* 2007a) using this equation.

Development of laminar or turbulent flow within an internal domain depends primarily on the Reynolds number (Re), a non-dimensional quantity which briefly combines four parameters influencing the flow: fluid density (ρ) and viscosity (μ), average fluid velocity (u) and characteristic domain diameter (D).

$$Re = \rho \cdot u \cdot D / \mu$$

In the present study Re varied between 177–6379 for the five cases and was calculated at the needle inlet (Table 1). Re in the rest of the domain is probably lower, owing to the fact that as the flow area increases, the velocity has to decrease, due to mass conservation

(Kurtcuoglu *et al.* 2007). Calculated values are considered low or moderate and characterize the flow as laminar or transitional.

The assumption of smooth walls on both the root canal and the needle is inconsistent with real dentine anatomy and to the findings of a previous study (Boutsioukis *et al.* 2007b). Wall roughness does not affect laminar flow that was observed in the middle and coronal third of the canal. Conversely it increases the resistance when the flow is turbulent, such as the one observed near the needle outlet in some cases, modifying the flow pattern. This effect depends on the relative height of the irregularities compared to the domain diameter and on the Re (McCabe *et al.* 2004).

It has been recommended that upon completion of canal preparation the canal contents should be flushed by means of a small-diameter irrigation needle (27 or 30G), with a safety tip (side-vented) placed in the apical third of the canal, even to working length or 1 mm short of it (Abou-Rass & Piccinino 1982, Zehnder 2006). Small-diameter irrigation needles seem to be more effective because they can reach further into the canal and thus may result in better exchange and cleaning (Senia *et al.* 1971, Chow 1983), as the overall effectiveness of irrigation is largely determined by the relative diameter of the irrigating needle and the canal (Ram). Small-diameter needles (30G) have been also

reported to provide significantly better irrigant exchange than larger-diameter needles (Druttman & Stock 1989). A 30-gauge side-vented needle with a safety tip was employed in this study.

The release of mass-less particles within the flow (Fig. 6) is considered a procedure that aids enhanced visualization of the flow pattern. Such particles are expected to follow the path of the fluid with accuracy (Tilton 1999, Fluent Inc. 2005). Mass-less particle trajectories do not represent paths of dentine shavings, which have very different densities from the irrigant. However, they might represent possible paths of microbes, which have densities very similar to the irrigant and limited volume.

Irrigant replacement in any part of the flow domain can be accomplished solely by flow of the irrigant already present in the canal towards the canal orifice, which is depicted by the magnitude of velocity along the longitudinal axis of the root canal (z-component of velocity). Therefore, the distribution of z-velocity along the longitudinal axis of the root canal (z-axis) indicates the amount of irrigant replacement occurring at different levels of the root canal (Fig. 7).

The effect of flow rate on the irrigant replacement, as depicted by the results of this study appears significant. Minimum irrigant replacement in the apical third that was limited to less than 1 mm apically to the needle tip was identified in cases A–C through analysis of streamlines (Fig. 6) and z-velocity distribution (Fig. 7). Irrigant replacement extended to 1–1.5 mm apically to the needle tip in cases D and E. It is possible that increasing inlet velocity as well as increasing amounts of turbulence developed enhanced irrigant replacement in the cases studied. However, cases A–C model the effect of the vast amount of flow rates used by clinicians, whilst cases D and E model extreme flow rate conditions rarely encountered in clinical practice (Boutsoukis *et al.* 2007a). Therefore, the requirement for placement of the needle tip to within 1 mm from working length (Abou-Rass & Piccinino 1982, Zehnder 2006) should be stressed.

Turbulence intensity and turbulent viscosity ratio depict the amount of turbulence developed in a flow field and whether it significantly influences the resulting flow. When examining wall-bounded flows with the RANS approach, turbulent viscosity ratios over 100 are generally considered to indicate a fully developed turbulent flow (Fluent Inc. 2005). Such condition could not be identified in any of the cases studied. Turbulent flow, by means of the chaotic eddy motion associated with velocity fluctuation, is conducive to

rapid mixing and, therefore, is the preferred flow regime for mixing (Tilton 1999). Such mixing of fresh irrigant with the irrigant already inside the root canal is necessary to ensure maximum irrigant replacement and efficiency in debridement and antibacterial activity (Salzgeber & Brilliant 1977).

An early attempt to simulate *in vitro* the irrigation of root canals and quantify the constant replenishment of the irrigant in primary and secondary canals during ultrasonic and sonic agitation led to the conclusion that irrigant cannot be adequately exchanged with new solution, even in secondary canals with diameters in the range of 1 mm. Moreover, it was verified that flow rate of the irrigant poses a significant effect on irrigant replacement throughout the canal (Nanzer *et al.* 1989). Results of the present study confirmed that irrigant flow rate significantly influences the flow pattern within the root canal.

Controversial results have been published regarding the extent of irrigant exchange apically to the tip of a side-vented needle. It has been reported that the solution does not reach further than 1 mm apically from the needle tip of 30G needles during irrigation (Zehnder 2006). The present results are consistent with that study, regarding the use of flow rates in the range of 0.02–0.26 mL sec⁻¹ (cases A–C). However, another study concluded that the zones of clearance beyond the tip of side-vented needles (25, 28 and 30G) were significant, indicating that highly effective canal clearance occurred without having to place the tip of the needle at the apical foramina. Moreover the effectiveness of these needles seemed related to their design, creating turbulence around and beyond the end of the needle (Kahn *et al.* 1995). According to the present findings, such irrigant replacement occurred only when flow rates in the range of 0.53–0.79 mL sec⁻¹ were used (cases D and E), values that do not represent average clinical conditions (Boutsoukis *et al.* 2007a). Neither of these studies reported flow rate of the irrigant used or whether it was standardized.

Stagnant behaviour of the irrigant within the most distal part of the needle lumen was detected in all cases studied. This observation questions the needle design, as irrigant stagnation could favor crystal accumulation within the needle lumen (McCabe *et al.* 2004). A possible explanation would be to avoid forceful extrusion of the irrigant to the periapical tissue in case of needle binding to the canal wall.

Results of the present study cannot be extrapolated to narrower root canals. In such a canal the effect of

any presently available irrigation system may be limited. Intermittent agitation of the canal content with a small size instrument (Druttman & Stock 1989, Kahn *et al.* 1995, Spangberg & Haapasalo 2002) or a gutta-percha cone (Huang *et al.* 2008, McGill *et al.* 2008) have been proposed to improve canal cleanliness. Further studies are needed to determine the flow pattern in narrow and curved root canals.

Thus, in terms of replacement efficiency, according to the results of the present study a flow rate of 0.01–0.26 mL sec⁻¹ should be combined with placement of the irrigation needle to within 1 mm from working length, in order to achieve acceptable irrigant exchange. Flow rates of 0.53–0.79 mL sec⁻¹ offer an additional advantage of 0.5 mm but cannot be regarded as average clinical conditions. Acceptable values might vary when different canal anatomy or different needles are considered.

Conclusions

Irrigant flow rate appears to be highly significant in determining the flow pattern within the root canal. Irrigant replacement apical to the needle tip was not satisfactory for any of the flow rates studied. Development of turbulent flow is desired as it leads to more efficient irrigant replacement. Computational Fluid Dynamics represents a powerful tool for the study of irrigations.

This study was submitted as a Dissertation to the Department of Endodontology, Dental School, Aristotle University of Thessaloniki, in partial fulfillment of the requirements for the Postgraduate Degree of Specialization in Endodontology.

References

- Abou-Rass M, Piccinino MV (1982) The effectiveness of four clinical irrigation methods on the removal of root canal debris. *Oral Surgery Oral Medicine Oral Pathology* **54**, 323–8.
- Arvand A, Hormes M, Reul H (2005) A validated computational fluid dynamics model to estimate hemolysis in a rotary blood pump. *Artificial Organs* **29**, 531–40.
- Boutsioukis C, Lambrianidis T, Kastrinakis E, Bekiaroglou P (2007a) Measurement of pressure and flow rates during irrigation of a root canal ex vivo with three endodontic needles. *International Endodontic Journal* **40**, 504–13.
- Boutsioukis C, Lambrianidis T, Vasiliadis L (2007b) Clinical relevance of standardization of endodontic irrigation needle dimensions according to the ISO 9626:1991 & 9626:1991/ Amd 1:2001 specification. *International Endodontic Journal* **40**, 700–6.
- Chow TW (1983) Mechanical effectiveness of root canal irrigation. *Journal of Endodontics* **9**, 475–9.
- Corno AF, Prosi M, Fridez P, Zunino P, Quarteroni A, von Segesser LK (2006) The non-circular shape of FloWatch® - PAB prevents the need for pulmonary artery reconstruction after banding. Computational fluid dynamics and clinical correlations. *European Journal of Cardiothoracic Surgery* **29**, 93–9.
- Druttman ACS, Stock CJR (1989) An in vitro comparison of ultrasonic and conventional methods of irrigant replacement. *International Endodontic Journal* **22**, 174–8.
- Falk KW, Sedgley CM (2005) The influence of preparation size on the mechanical efficacy of root canal irrigation in vitro. *Journal of Endodontics* **31**, 742–5.
- Fluent Inc. (2005) *Fluent 6.2: User's guide*. Lebanon, USA: Fluent Inc., pp. 11.1–88, 29.1–152.
- Goldman M, Kronman JH, Goldman LB, Clausen H, Grady J (1976) New method of irrigation during endodontic treatment. *Journal of Endodontics* **2**, 257–60.
- Guerisoli DMZ, Silva RS, Pecora JD (1998) Evaluation of some physico-chemical properties of different concentrations of sodium hypochlorite solutions. *Brazilian Endodontic Journal* **3**, 21–3.
- Gulabivala K, Patel B, Evans G, Ng YL (2005) Effects of mechanical and chemical procedures on root canal surfaces. *Endodontic Topics* **10**, 103–22.
- Haapasalo M, Endal U, Zandi H, Coil JM (2005) Eradication of endodontic infection by instrumentation and irrigation solutions. *Endodontic Topics* **10**, 77–102.
- Hsieh YD, Gau CH, Kung Wu SF, Shen EC, Hsu PW, Fu E (2007) Dynamic recording of irrigating fluid distribution in root canals using thermal image analysis. *International Endodontic Journal* **40**, 11–7.
- Huang TY, Gulabivala K, Ng YL (2008) A bio-molecular film ex-vivo model to evaluate the influence of canal dimensions and irrigation variables on the efficacy of irrigation. *International Endodontic Journal* **41**, 60–71.
- Hughes WF, Brighton JA (1999) *Fluid dynamics*, 3rd edn. New York, USA: McGraw-Hill. pp. 2–6, 34–61, 118–23, 245–6.
- Ingle JI, Himel VT, Hawrish CE *et al.* (2002) Endodontic cavity preparation. In: Ingle JI, Bakland LK, eds. *Endodontics*, 5th edn. Ontario, Canada: BC Decker, pp. 502.
- Jung J, Lyczkowski RW, Panchal CB, Hassanein A (2006) Multiphase hemodynamic simulation of pulsatile flow in a coronary artery. *Journal of Biomechanics* **39**, 2064–73.
- Kahn FH, Rosenberg PA, Gliksberg J (1995) An in vitro evaluation of the irrigating characteristics of ultrasonic and subsonic handpieces and irrigating needles and probes. *Journal of Endodontics* **21**, 277–80.
- Krell KV, Johnson RJ, Madison S (1988) Irrigation patterns during ultrasonic canal instrumentation. Part I. K-type files. *Journal of Endodontics* **14**, 65–8.

- Kurtcuoglu V, Soellinger M, Summers P et al. (2007) Computational investigation of subject-specific cerebrospinal fluid flow in the third ventricle and aqueduct of Sylvius. *Journal of Biomechanics* **40**, 1235–45.
- Lambrianidis TP (2001) *Risk management in root canal treatment*, 1st edn. Thessaloniki, Greece: University Studio Press, pp. 163–73.
- Lambrianidis T, Tosounidou E, Tzoanopoulou M (2001) The effect of maintaining apical patency on periapical extrusion. *Journal of Endodontics* **27**, 696–8.
- Lee SJ, Wu MK, Wesseling PR (2004a) The effectiveness of syringe irrigation and ultrasonics to remove debris from simulated irregularities within prepared root canal walls. *International Endodontic Journal* **37**, 672–8.
- Lee SJ, Wu MK, Wesseling PR (2004b) The efficacy of ultrasonic irrigation to remove artificially placed dentine debris from different-sized simulated plastic root canals. *International Endodontic Journal* **37**, 607–12.
- McCabe WL, Smith JC, Harriott P (2004) *Unit operations of chemical engineering*, 7th edn. New York, USA: McGraw-Hill, pp. 45–67, 98–132, 244–98, 929–65.
- McGill S, Gulabivala N, Mordan N, Ng YL (2008) The efficiency of dynamic irrigation using a commercially available system (RinsEndo[®]) determined by removal of a collagen 'bio-molecular film' from an ex vivo model. *International Endodontic Journal* **41**, 602–8.
- Moser JB, Heuer MA (1982) Forces and efficacy in endodontic irrigation systems. *Oral Surgery Oral Medicine Oral Pathology* **53**, 425–8.
- Nanzer J, Langlois S, Coeuret F (1989) Electrochemical engineering approach to the irrigation of tooth canals under the influence of a vibrating file. *Journal of Biomedical Engineering* **11**, 157–63.
- Nguy D, Sedgley C (2006) The influence of canal curvature in the mechanical efficacy of root canal irrigation in vitro using real-time imaging of bioluminescent bacteria. *Journal of Endodontics* **32**, 1077–80.
- Pekkan K, De Zelicourt D, Ge L et al. (2005) Physics-driven CFD modeling of complex anatomical cardiovascular flows – a TCPC case study. *Annals of Biomedical Engineering* **33**, 284–300.
- Peters OA (2004) Current challenges and concepts in the preparation of root canal systems: a review. *Journal of Endodontics* **30**, 559–67.
- Politis AK, Stavropoulos GP, Christolis MN, Panagopoulos FG, Vlachos NS, Markatos NC (2007) Numerical modeling of simulated blood flow in idealized composite arterial coronary grafts: steady state simulations. *Journal of Biomechanics* **40**, 1125–36.
- Ponce EE, Fernandez JAV (2003) The cemento-dentino-canal junction, the apical foramen, and the apical constriction: evaluation by optical microscopy. *Journal of Endodontics* **29**, 214–9.
- Ram Z (1977) Effectiveness of root canal irrigation. *Oral Surgery Oral Medicine Oral Pathology* **44**, 306–12.
- Ruddle CJ (2002) Cleaning and shaping the root canal. In: Cohen S, Burns RC, eds. *Pathways of the pulp*, 8th edn. St. Louis, USA: Mosby, pp. 258–62.
- Salzgeber MR, Brilliant DJ (1977) An in vivo evaluation of the penetration of an irrigating solution in root canals. *Journal of Endodontics* **3**, 394–8.
- Sedgley C, Applegate B, Nagel A, Hall D (2004) Real-time imaging and quantification of bioluminescent bacteria in root canals in vitro. *Journal of Endodontics* **30**, 893–8.
- Sedgley CM, Nagel AC, Hall D, Applegate B (2005) Influence of irrigant needle depth in removing bacteria inoculated into instrumented root canals using real-time imaging in vitro. *International Endodontic Journal* **38**, 97–104.
- Senia ES, Marshall JF, Rosen S (1971) The solvent action of sodium hypochlorite on pulp tissue of extracted teeth. *Oral Surgery Oral Medicine Oral Pathology* **31**, 96–103.
- van der Sluis LWM, Wu MK, Wesseling PR (2005) The efficacy of ultrasonic irrigation to remove artificially placed dentine debris from human root canals prepared using instruments of varying taper. *International Endodontic Journal* **38**, 764–8.
- van der Sluis LWM, Gambarini G, Wu MK, Wesseling PR (2006) The influence of volume, type of irrigant and flushing method on removing artificially placed dentine debris from the apical root canal during passive ultrasonic irrigation. *International Endodontic Journal* **39**, 472–6.
- Spangberg LSW, Haapasalo M (2002) Rationale and efficacy of root canal medicaments and root filling materials with emphasis on treatment outcome. *Endodontic Topics* **2**, 35–8.
- Tilton JN (1999) Fluid and particle dynamics. In: Perry RH, Green DW, Maloney JO, eds. *Perry's chemical engineer's handbook*, 7th edn. New York, USA: McGraw-Hill, pp. 6.1–50.
- Tinaz AC, Alacam T, Uzun O, Maden M, Kayaoglu G (2005) The effect of disruption of apical constriction on periapical extrusion. *Journal of Endodontics* **31**, 533–5.
- van Tricht I, De Wachter D, Tordoir J, Verdonck P (2006) Comparison of the hemodynamics in 6 mm and 4–7 mm hemodialysis grafts by means of CFD. *Journal of Biomechanics* **39**, 226–36.
- Vande Visse JE, Brilliant JD (1975) Effect of irrigation on the production of extruded material at the root apex during instrumentation. *Journal of Endodontics* **1**, 243–6.
- Wesseling P, Bergenholtz G (2004) Treatment of the necrotic pulp. In: Bergenholtz G, Horsted-Bindslev P, Reit C, eds. *Textbook of endodontology*, 1st edn. Oxford, UK: Blackwell Munksgaard, pp. 163–4.
- Xu C, Sin SH, McDonough JM et al. (2006) Computational fluid dynamics modeling of the upper airway of children with obstructive sleep apnea syndrome in steady flow. *Journal of Biomechanics* **39**, 2043–54.
- Yang XL, Liu Y, Luo HY (2006a) Respiratory flow in obstructed airways. *Journal of Biomechanics* **39**, 2743–51.

- Yang XL, Liu Y, So RMC, Yang JM (2006b) The effect of inlet velocity profile on the bifurcation COPD airway flow. *Computers in Biology and Medicine* **36**, 181–94.
- Yoganathan P, Chandran KB, Sotiropoulos F (2005) Flow in prosthetic heart valves: state-of-the-art and future directions. *Annals of Biomedical Engineering* **33**, 1689–94.
- Zehnder M (2006) Root canal irrigants. *Journal of Endodontics* **32**, 389–98.